HHS Public Access

Author manuscript

J Neurooncol. Author manuscript; available in PMC 2020 January 01.

Published in final edited form as:

J Neurooncol. 2019 January ; 141(1): 111–120. doi:10.1007/s11060-018-03013-x.

Imaging Tryptophan Uptake with Positron Emission Tomography in Glioblastoma Patients Treated With Indoximod

Rimas V Lukas, MD[1,3,4], **Csaba Juhász, MD, PhD**[5,6], **Derek A Wainwright, PhD**[2,3,4], **C David James, PhD**[2,3,4], **Gene Kennedy, MD**[7], **Roger Stupp, MD**[1,2,3,4], and **Maciej S Lesniak, MD**[2,3,4]

[1]Department of Neurology, Northwestern University

[2]Department of Neurosurgery

[3]Lurie Cancer Center

[4]Malnati Brain Tumor Institute

[5]Wayne State University, Department of Pediatrics, Neurology, and Neurosurgery

[6]Karmanos Cancer Institute

[7]NewLink Genetics

Abstract

Introduction: Glioblastoma (GBM) is the most frequent and aggressive primary tumor of the central nervous system (CNS), accounting for over 50% of all primary malignant gliomas arising in the adult brain. Even after surgical resection, adjuvant radiotherapy (RT) and temozolomide (TMZ) chemotherapy, as well as tumor-treating fields, the median survival is only 15–20 months. We have identified a pathogenic mechanism that contributes to the tumor-induced immunosuppression in the form of increased indoleamine 2,3 dioxygenase 1 (IDO1) expression; an enzyme that metabolizes the essential amino acid, tryptophan (Trp), into kynurenine (Kyn). However, real-time measurements of IDO1 activity has yet to become mainstream in clinical protocols for assessing IDO1 activity in GBM patients.

Methods: Pre-treatment and on-treatment α-[^{11}C]-methyl-*L*-Trp (AMT) positron emission tomography (PET) with co-registered MRI was performed on patients with recurrent GBM treated with the IDO1 pathway inhibitor indoximod (*D*1-MT) and temozolomide.

Results: Regional intratumoral variability of AMT within enhancing and non-enhancing tumor was noted at baseline. On treatment imaging revealed decreased regional uptake suggesting IDO1 pathway modulation with treatment.

Conclusions: Here, we have validated the ability to use PET of the Trp probe, AMT, for use in visualizing and quantifying intratumoral Trp uptake in GBM patients treated with an IDO1

Corresponding author: Rimas V. Lukas, MD, 710 N. Lake Shore Drive, Abbott Hall 1114, Chicago, IL 60611, (312) 695-0990, (312) 695-1435 (fax), rimas.lukas@nm.org.

COMPLIANCE WITH ETHICAL STANDARDS

G. Kennedy is an employee of New Link Genetics. All other authors report no conflicts of interest. This research was conducted in compliance with the ethical standards of the institutional research committees and with the 1964 Helsinki declaration and its later amendments or comparable ethical standards. All patients provided signed informed consent for participation in this research.

pathway inhibitor. These data serve as rationale to utilize AMT-PET imaging in the future evaluation of GBM patients treated with IDO1 enzyme inhibitors.

Keywords

AMT; biomarker; glioblastoma; IDO; 1-MT; PET

INTRODUCTION

Glioblastoma (GBM) is the most common malignant primary brain tumor in adults.[1] The standard of care management for newly diagnosed GBM includes surgery, radiation, temozolomide chemotherapy, and tumor treating fields.[2,3] For recurrent or progressive disease, the optimal management is less clearly defined.[4] Therapies for progressive GBM are being actively investigated. The role of immunotherapies for progressive disease is an area of particularly intense exploration.[5,6]

With respect to the increasing prevalence of testing immunotherapeutic strategies in clinical trials for cancer patients, there have been a number of challenges associated with the interpretation of radiographic imaging and its relevance to the patient's responsiveness to treatment efficacy.[7] Contemporary criteria have been developed to address this problem, including the Immune Response Assessment in Neuro-Oncology (iRANO)[8].This approach utilizes post-contrast and T2/FLAIR MRI sequences. Advancements of imaging modalities that distinguish a specific response due to treatment, versus the non-specific contributions due to disease progression, would be of particularly high value for patients with intracranial tumors and treated with immunotherapy. Accordingly, an early confirmation that a patient was responding to an immunotherapeutic modality would prevent the unnecessary continuation of ineffective treatments, even while the patients may undergo progressive worsening according to conventional imaging results and/or symptoms associated with clinical worsening.

The enzyme, indoleamine 2,3 dioxygenase (IDO1), is an attractive immunologic target for the treatment of GBM due to its high level of expression [9] and potently immunosuppressive activity [10]. IDO1 converts tryptophan (Trp) into kynurenine (Kyn), and depletion of Trp [11] or the accumulation of Kyn, have been demonstrated to suppress T cell effector functions and/or increase conversion of naïve $CD4^+$ T cells into $FoxP3^+$ regulatory T cells (Tregs) [12]. In animal models, the genetic suppression of IDO1 in mouse GBM cells leads to the loss of intra-glioma Treg accumulation and a substantial long-term T cell-mediated survival benefit [10,13]. The oral IDO1 pathway inhibitor, indoximod (*D*1-MT), has been assessed for its safety when used in conjunction with cytotoxic chemotherapy.[14] Co-administration of indoximod with temozolomide has demonstrated a synergistic survival benefit in mouse models with intracranial brain tumors [13,15], and this approach is under clinical investigation in progressive high-grade glioma patients [16–20]. The preclinical validation that, IDO1 enzyme inhibitors possess beneficial survival effects [21]coupled with the high safety and tolerability of this drug class among early-phase clinical trials [22,23], has stimulated the development of imaging approaches that quantify tryptophan uptake activity. One such approach involves the study of α-[^{11}C]-methyl-*L*-Trp

(AMT), a tryptophan analog that allows for quantification of tryptophan metabolism [24–31]. The uptake of AMT can be detected in both contrast-enhancing and biopsy-proven non-enhancing tumor [31,32]. Positron emission tomography of AMT uptake rates are suggestive of a correlation with intratumoral IDO1 expression as confirmed by the analysis of post-treatment resected tissue [33]. In progressive GBM patients evaluated with the AMT-PET method, a higher intratumoral AMT rate of uptake was associated with shorter survival [34]. The conclusions of Kamson et al. are based on the analysis of a single time point for each patient, although serial imaging of tumor for assessing the response to therapy has been reported in a limited number of patients [35]. Here, we report the initial results from a multi-time point AMT-PET imaging study for three GBM patients, with imaging prior to- and while on-treatment with the IDO1 pathway inhibitor, indoximod.

METHODS

Clinical Studies

We conducted a prospective pilot study of AMT-PET imaging in patients with recurrent or progressive GBM treated with the Trp mimetic, indoximod, in a phase 1/2 clinical trial. For patients who were enrolled in the phase II portion of the trial, additional AMT-PET imaging, prior to treatment initiation and after ~2 months on therapy, was offered. Standard MRI for formal treatment evaluation was obtained at baseline and every 2 months thereafter. Treatment consisted of oral indoximod 1200mg twice daily provided with concurrent temozolomide 150 mg/m2 (5/28 days).

The clinical trial was listed at clinicaltrials.gov under the identifier NCT02052648. The imaging study was approved by the Institutional Review Boards of the University of Chicago and Wayne State University. All patients provided informed consent for participation in the trial and separate informed consents were received for individuals desiring additional AMT-PET imaging study.

PET Imaging Acquisition

AMT-PET studies were performed using a GE Discovery STE PET/CT scanner with a 15 cm field of view which generates 47 image planes with a slice thickness of 3 mm. The reconstructed image resolution is 7.5 ± 0.4 mm (isotropic), and images from this scanner were iteratively reconstructed (2 iterations, 16 subsets, 8 mm axial smoothing). AMT tracer was synthesized using a standard method [36]. A previously described scanning procedure was utilized [31]. Patients fasted for 6 hours prior to AMT PET to facilitate a low plasma concentration of Trp and other large neutral amino acids. A venous line was established for injection of AMT (0.1 mCi/kg) as a slow bolus. A second venous line was established for collection of timed blood samples (0.5 mL/sample, collected at 0, 20, 30, 40, 50 and 60 min after AMT injection). Blood radioactivity data was used for Patlak graphical analysis (see below).

Following injection of AMT, a 20-minute dynamic PET scan of the heart was performed (sequence: 12×10 s, 3×60 s, and 3×300 s) in 2D-mode to obtain left ventricular (LV) blood input function. Continuation of blood input function beyond the initial 20 minutes was then

achieved using venous blood samples obtained during brain scanning. Twenty-five minutes after tracer injection, a 5-minute CT scan of the brain was followed by a 35-min dynamic emission, high-sensitivity 3D PET scan of the brain (7 × 5 minutes). Measured attenuation correction, scatter, and decay correction were applied to all PET images. Plasma samples were obtained and counted in a NaI well counter, cross-calibrated to the PET scanner, in order to obtain the blood input function.

PET Image Analysis.

Co-registration of PET and MRI image volumes.—Multimodal image co-registration and analysis were performed utilizing 3D Slicer software (www.slicer.org) [37,38]. Images were co-registered with pre- and post-contrast axial T1 MR images, T2 and FLAIR images using the Fast Rigid Registration module.[39] Fused images were automatically resliced and resampled. MRI abnormalities on the post-contrast images were delineated semi-automatically, and the volumes of interest (VOI) were used for quantitative assessment of AMT uptake and kinetic parameters.

Quantitative assessment of AMT tumor uptake.—In all three patients, the tumoral AMT uptake in volumes-of-interest (VOIs), defined on the contrast-enhanced MRI, were characterized by standardized uptake values (SUVs). The SUV calculation relates tracer concentration in tissue to the dose injected and the subject's mass [40] (SUV= tissue concentration in ROI [uCi/cc]/injected dose per weight [mCi/kg]). Since all subjects received the same injected dose based upon weight (0.1 mCi/kg), the SUV images were directly obtained by averaging dynamic brain image sequence obtained 30–55min after tracer injection, during which time metabolic product is the highest. Tumoral SUVs were normalized by dividing their values by SUV measured in normal contralateral cortex, thus creating a tumor/cortex SUV ratio. Based on our previous studies, SUV tumor/cortex ratios 1.65 and above are consistent with recurrent GBM (rGBM) [28,34].

In patient 2, where full kinetic PET data and blood data were available for both pre- and on-treatment AMT-PET images, we also performed tracer kinetic analysis by using a Patlak graphical analysis, as described before [31,32,41]. This analysis yields the AMT K value (among other parameters), and the calculated k_3 value, parameters used as an imaging correlate of tracer trapping and tumoral conversion of Trp via the Kyn pathway [24,33,42].

Comparison of AMT uptake between baseline and follow-up AMT-PET images.—Baseline and follow-up (post-treatment) AMT-PET images were co-registered, together with corresponding (clinically acquired) 3 T MR images, obtained within one week of the PET images. VOIs created on the baseline images were transferred to the post-treatment images to ensure that AMT uptake and kinetic parameters were measured repeatedly in the same tumor volume for comparison. AMT SUVs and tumor/cortex SUV ratios, as well as K and K ratios (for patient #2), were calculated from both the baseline and post-treatment PET images and compared to each other. The changes in AMT uptake were also compared to interval changes in tumoral contrast enhancement and FLAIR signal changes as defined by the RANO criteria [43].

RESULTS

Three patients with recurrent primary GBM enrolled in the ancillary study. Their individual characteristics and treatment course are summarized in table 1 and described immediately below. Patients received TMZ and indoximod as per protocol for 2 or more cycles.

Patient 1

Patient #1 was a 36 year old with IDH wild type (IDHwt), MGMT promoter unmethylated GBM. After treatment with standard radiochemotherapy, she was surgically treated again with resection of recurrent tumor. She underwent a post-operative pre-treatment MRI and AMT-PET. The patient completed two 28-day cycles of indoximod and temozolomide, followed by reimaging with MRI and AMT-PET. The patient initiated treatment on-study with 2mg dexamethasone, daily, which was further increased to 12mg, daily, for symptoms associated with headaches, nausea, and weakness. The patient was taken off study after 2 cycles due to clinical and radiographic progression. The patient died of disease progression 5 and ½ months after initiating concurrent indoximod and temozolomide treatment.

On-treatment MRI demonstrated progression of both enhancing and FLAIR lesions (Figure 1) with associated clinical decline necessitating higher steroid doses. Different regions of the enhancing lesion demonstrated distinct findings with respect to AMT-PET uptake. In the posterior component of the lesion, there was increased AMT uptake at baseline (SUV ratio 1.65), consistent with active tumor, while the medial component showed low AMT uptake (Figure 1). After treatment with the IDO1 pathway inhibitor, a decrease of AMT uptake was evident in the posterior portion: a result suggesting some effects due to therapeutic intervention. Surprisingly, a large increase in uptake of AMT was evident in the medial portion (from 1.28 to 2.10 SUV ratio), along with the expansion of the contrast-enhancing area, suggesting progression for this portion of the tumor.

Patient 2

Patient #2 was 63 years old, with IDHwt, MGMT promoter methylated GBM, and who received standard radiochemotherapy for initial treatment of primary tumor. Upon determination of tumor progression, the patient underwent pretreatment MRI and AMT-PET. He then received 2 cycles of indoximod and temozolomide followed by on-treatment AMT-PET. There was clinical and radiographic progression at one month following a 3rd cycle of indoximod and temozolomide, at which point the patient was taken off study and received further lines of treatment. He is alive 18 months after initiation of indoximod with temozolomide therapy for progressive disease. He was not provided steroids during the course of study treatment.

On-treatment MRI demonstrated progression in the enhancing lesions (Figure 2) and surrounding areas of increased FLAIR signal. This correlated with the development of aphasia which continued to progress after AMT-PET imaging, and resulted in the patient being taken off study. Initial AMT-PET results revealed a higher SUV ratio in the posterior nodule than in the anterior-lateral contrast-enhancing mass (2.33 vs. 1.72), with both results providing consistency with tumor burden (Figure 2). On-treatment AMT-PET showed stable

AMT uptake in the larger anterior mass despite progression on MRI (suggesting pseudo-progression), while the SUV ratio showed a mild increase in the posterior nodule (to 2.5), a less than 10% change that could be intrasubject variability. PET kinetic analysis showed a more robust interval decrease in AMT K ratios in both lesions (2.04 to 1.6 in the anterior, and 1.27 to 1.14 in the posterior lesion): a result suggesting decreased AMT metabolic rates and potentially associated with IDO1 pathway modulation. Tumor/cortex k_3 ratios also decreased. The length of survival for this patient (>18 months after 2nd progression) suggests that the clinical and MRI results may have reflected pseudoprogression, and that the patient's tumor may have responded to IDO pathway inhibitor treatment.

Patient 3

Patient #3 was a 46 year old with IDHwt, MGMT promoter unmethylated GBM, and received radiochemotherapy plus tumor treating fields following the initial surgery. Upon progression, he underwent a pre-treatment MRI and AMT-PET, and then initiated indoximod and temozolomide treatment. He developed a rapid clinical progression with radiographic indication of cerebrospinal fluid dissemination, following 1 cycle of treatment for recurrent tumor. Pre-treatment MRI or AMT-PET imaging results did not show evidence of CSF dissemination. Due to the rapid clinical decline, the patient did not undergo repetitive on-treatment imaging. The patient was taken off study following the initial cycle of treatment and died 2 months after beginning indoximod with temozolomide.

Pre-treatment MRI and AMT-PET results showed regions of variable AMT uptake within the enhancing lesion, and SUV ratios consistent with active tumor (1.73) (Figure 3).

DISCUSSION

In the current study, we evaluated 3 patients diagnosed with recurrent IDHwt GBM with variable MGMT methylation status and treated with a combination of the Trp mimetic, indoximod, and temozolomide. No objective responses were demonstrated, although the results from our analysis provide new information and observations that warrant further consideration, including: (i) heterogeneous intratumoral tryptophan uptake in recurrent GBM patients, potentially reflecting IDO activity; (ii) AMT-PET imaging as a biomarker for evaluating the GBM patient response to indoximod; and (iii) AMT-PET as a future modality for distinguishing pseudoprogression as compared to true progression, in patients treated with indoximod.

MRI post-contrast imaging is known to be impacted by tumor, as well as by acute and delayed effects of radiation and systemic therapy. With systemic therapies, progressive enhancement in the setting of no true tumor growth (i.e., pseudoprogression) has been reported with traditional alkylating agents [44], as well as with immunotherapies [45, 46]. Intense, treatment-induced inflammation may lead to progressive MRI changes as a result of immune checkpoint inhibitor therapy [46]. While a widely acknowledged phenomenon, the incidence of GBM pseudoprogression in relation to immunotherapies is unknown. It is reasonable to assume that the incidence and the timing of pseudoprogression will vary between the specific immunotherapy(s) used. It would also be expected that the use of alkylating agents in MGMT promoter methylated patients, tumor-intrinsic factors (i.e.,

molecular profile) as well as treatment-specific factors (steroid use) could influence the likelihood of pseudoprogression developing.

PET imaging is particularly attractive as a non-invasive, quantitative assessment of therapeutic activity and/or responsiveness to immunotherapeutic strategies for patients diagnosed with malignant glioma. Fluorodeoxyglucose (FDG) PET has been the modality most frequently utilized in clinical imaging of malignancy. Its role is undergoing investigation in recurrent GBM [47]. Other PET probes are also under investigation. A recent study demonstrated the feasibility of PET probes targeting deoxycytidine kinase to evaluate immune cell aggregation in gliomas [48]. While this technique requires further evaluation in a clinical setting, amino acid PET is currently available to patients and has shown the ability to differentiate between pseudoprogression and GBM recurrence [49]. The effectiveness of IDO1 enzyme inhibitors to substantially block the conversion of Trp into Kyn may be further supported by assessments of intratumoral AMT uptake. The prognostic utility of AMT-PET imaging at a single time point in patients with progressive grade 3 and 4 gliomas has been previously demonstrated [34]. Increased intratumoral AMT (SUV_{mean} and SUV_{max}) at the time of recurrence, but prior to initiation of treatment for recurrent disease, was associated with shorter survival. Serial AMT-PET imaging has also been performed in several patients with recurrent GBM, prior to- and actively receiving-tumor treating fields therapy, and has demonstrated an interval decrease in intratumoral AMT uptake as a potential indication of a response to treatment. Some of the AMT-PET changes occurred prior to responses observed by conventional MRI imaging [35]. Thus, an interval decrease in AMT uptake ratios during indoximod treatment is unlikely to be associated with tumor progression, even if MRI showed progressive contrast enhancement.

Our study is in-line with previous observations and suggests that, the treatment of rGBM patients with the Trp mimetic, indoximod, provides an impact on AMT-PET imaging in the tumor. A limitation of our current study is that the static PET images do not differentiate between tracer uptake versus trapping changes, directly related to transport versus metabolic activity, respectively. However, the results for patient #2 were particularly interesting, since we were able to quantify tracer kinetics, before and after treatment with indoximod. Patient #2 showed the highest baseline SUV tumor/cortex ratio, which is a negative prognostic factor [34], along with MRI signs suggestive of on-treatment progression. However, AMT uptake showed an interval decrease, with kinetic comparisons suggestive of a decreased metabolism of Trp. Interestingly, Patient #2 also possessed the longest OS of the three patients in our study and supports future serial imaging of GBM with AMT-PET for patients receiving IDO1 pathway blockade therapy. However, the potential for AMT-PET to serve as a predictive biomarker for GBM response to immunotherapy requires future validation in a prospective trial.

A minor limitation of utilizing AMT-PET to image IDO1-associated Trp uptake is that, although intratumoral IDO1 metabolism is suspected to be a major factor associated with this process, it’s notable that additional enzymes associated with Trp metabolism exist. Namely, tryptophan dioxygenase (TDO), as well as tryptophan hydroxylase 1 (TPH1) and TPH2, collectively possess the ability to convert Trp into downstream metabolites. Although TDO is highly expressed in a majority of patient-resected GBM [9,50] it’s considered to be

an unlikely contributor to AMT uptake, based on the high specificity for unmodified *L*-Trp [51,52]. In contrast, AMT is readily converted by TPH enzyme [53], and while the expression levels for the serotonergic pathway catalysts are currently unknown in GBM, they are the subject of an ongoing investigation. Moving forward, clinical study designs combining AMT-PET imaging, kinetic analyses of both tumor and serum for Trp and Kyn levels, as well as the use of an IDO1 enzyme inhibitor, would provide better resolution to the differentiation between changes in AMT transport versus Trp metabolism, as well as its relationship to IDO1-specific enzyme activity. We will plan to pursue this within the context of a phase 1/2 trial of IDO inhibition in conjunction with radiotherapy and PD1 blockade in newly diagnosed GBM.

ACKNOWLEDGEMENTS

Funding: M.S. Lesniak is supported by PHS grant numbers R01NS093903 awarded by the NIH/NINDS, and P50CA221747 awarded by the NIH/NCI, U.S. Department of Health and Human Services. R.V. Lukas is supported by PHS grant number R01NS093903 awarded by the NIH/NINDS and P50CA221747 awarded by the NIH/NCI, U.S. Department of Health and Human Services. D.A. Wainwright is supported by PHS grant number R01NS097851 awarded by the NIH/NINDS and P50CA221747 awarded by the NIH/NCI, U.S. Department of Health and Human Services. C. Juhasz is supported by PHS grant number R01NS093903 awarded by the NIH/NINDS, and R01CA123451 and P50CA221747 awarded by the NCI/NIH, U.S. Department of Health and Human Services. C.D. James is supported by PHS grant number P50CA221747 awarded by the NCI/NIH, U.S. Department of Health and Human Services. R. Stupp is supported by PHS grant number P50CA221747 awarded by the NIH/NCI, U.S. Department of Health and Human Services.

REFERENCES

1. Ostrum QT, Gittleman H, Xu J, et al. (2016) The CBTRUS Statistical Report: primary brain and central nervous system tumors diagnosed in the United States in 2009–2013. Neuro Oncol 18(suppl 5):v1–v75. [PubMed: 28475809]
2. Stupp R, Mason WP, van den Bent MJ, et al. (2005) Radiotherapy plus concomitant and adjuvant temozolomide for glioblastoma. N Engl J Med 352:987–996. [PubMed: 15758009]
3. Stupp R, Taillibert S, Kanner A, et al. (2017) Effect of tumor-treating fields plus maintenance temozolomide vs maintenance temozolomide alone on survival in patients with glioblastoma: a randomized clinical trial. JAMA 318:2306–2316. [PubMed: 29260225]
4. Lukas RV, Mrugala MM (2017) Pivotal trials for infiltrating gliomas and how they affect clinical practice. Neuro Oncol Practice 4:209–219.
5. Sampson JH, Maus MV, June CH (2017) Immunotherapy for brain tumors. J Clin Oncol 35:2450–2456. [PubMed: 28640704]
6. Binder DC, Davis AA, Wainwright DA (2015) Immunotherapy for cancer in the central nervous system: current and future directions. Oncoimmunology 5:e1082027. [PubMed: 27057463]
7. Huang RY, Neagu MR, Reardon DA, Wen PY (2015) Pitfalls in the neuroimaging of glioblastoma in the era of antiangiogenic and immuno/targeted therapy-detecting elusive disease, defining response. Front Neurol 6:33. [PubMed: 25755649]
8. Okada H, Weller M, Huang R, et al. (2015) Immunotherapy response assessment in neuro-oncology: a report of the RANO working group. Neuro Oncol. 16:e534–542.
9. Zhai L, Ladomersky E, Lauing KL, et al. (2017) Infiltrating T cells increase IDO1 expression in glioblastoma and contribute to decreased patient survival. Clin Cancer Res 23:6650–6660. [PubMed: 28751450]
10. Wainwright DA, Balyasnikova IV, Chang AL, et al. (2012) IDO expression in brain tumors increases the recruitment of regulatory T cellsand negatively impacts survival. Clin Cancer Res 18:6110–6121. [PubMed: 22932670]

11. Munn DH, Shafizadeh E, Attwood JT, Bondarev I, Pashine A, Mellor AL (1999) Inhibition of T cell proliferation by macrophage tryptophan catabolism. J Exp Med 189:1363–1372. [PubMed: 10224276]
12. Mezrich JD, Fechner JH, Zhang X, Johnson BP, Burlingham WJ, Bradfield CA (2010) An interaction between kynurenine and aryl hydrocarbon receptor can generate regulatory T cells. J Immunol 185:3190–3198. [PubMed: 20720200]
13. Wainwright DA, Chang AL, Dey M, et al. (2014) Durable therapeutic efficacy utilizing combinatorial blockade against IDO, CTLA-4, and PD-L1 in mice with brain tumors. Clin Cancer Res 20:5290–5301. [PubMed: 24691018]
14. Soliman HH, Jackson E, Neuger T, et al. (2014) A first in man phase I trial of the oral immunomodulator, indoximod, combined with docetaxel in patients with metastatic solid tumors. Oncotarget 5:8136–8146. [PubMed: 25327557]
15. Hanihara M, Kawataki T, Oh-Oka K, Mitsuka K, Nakao A, Kinouchi H (2016) Synergistic anti-tumor effect with indoelamine 2,3-dioxygenase inhibition and temozolomide in a murine glioma model. J Neurosurg 124:1594–1601. [PubMed: 26636389]
16. Colman H, et al. (2015) A phase 1b/2 study of the combination of the IDO pathway inhibitor indoximod and temozolomide for adult patients with temozolomide-refractory primary malignant brain tumors: Safety analysis and preliminary efficacy of the phase 1b component. J Clin Oncol 33(15_suppl):2070.
17. Zakharia Y, Colman H, Mott F, et al. (2015) Updates on phase 1B/2 combination study of the IDO pathway ihibitor indoximod with temozolomide for adult patients with temozolomide-refractory primary malignant brain tumors. Neuro Oncol 17:v112.
18. Zakharia Y, Munn D, Link C, Vahanian N, Kennedy E (2016) Interim analysis of phase 1B/2 combination study of the IDO pathway inhibitor indoximod with temozolomide for adult patients with temozolomide-refractory primary malignant brain tumors. ACTR-53. Neuro Oncol 18(Suppl_6):vi13–vi14.
19. Zhai L, Spranger S, Binder DC, et al. (2015) Molecular pathways: targeting IDO and other tryptophan dioxygenases for cancer immunotherapy. Clin Cancer Res 21:5427–5433. [PubMed: 26519060]
20. Zhai L, Ladomersky E, Lenzen A, et al. (2018) IDO1 in cancer: a gemini of immune checkpoints. Cell Mol Immunol. [EPub ahead of print]
21. Ladomersky E, Zhai L, Lenzen A, et al. (2018) IDO1 inhibition synergizes with radiation and PD1 blockade to durably increase survival against advanced glioblastoma. Clin Cancer Res. [EPub ahead of print]
22. Beatty GL, et al. (2017) First-in-Human Phase I Study of the Oral Inhibitor of Indoleamine 2,3-Dioxygenase-1 Epacadostat (INCB024360) in Patients with Advanced Solid Malignancies. Clin Cancer Res 23:3269–3276. [PubMed: 28053021]
23. Siu LL, Gelmon K, Chu Q, et al. (2017) BMS-986205 an optimized indoelamine 2,3-dioxygenase 1 (IDO1) inhibitor, is well tolerated with potent pharmacodynamics activity, alone and in combination with nivolumab in advanced cancers in a phase 1/2a trial. Abstract CT116. Cancer Res 77(13 Suppl) :CT116.
24. Chugani DC, Muzik O (2000) Alpha[C-11]methyl-L-tryptophan PET maps brain serotonin synthesis and kynurenine pathway metabolism. J Cereb Blood Flow Metab. 20(1):2–9. [PubMed: 10616786]
25. Madras BK, Sourkes TL (1965) Metabolism of alpha-methyltryptophan. Biochem Pharmacol 14:1499–1506. [PubMed: 5867505]
26. Diksic M, Nagahiro S, Sourkes TL (1990) Biological model for the in vivo measurement of rate of serotonin synthesis in the brain. J Neural Transm Suppl 29:131–140. [PubMed: 2358798]
27. Guastella AR, Michelhaugh SK, Klinger NV, et al. (2016) Tryptophan PET imaging of the kynurenine pathway in patient-derived xenograft models of glioblastoma. Mol Imaging. 15.
28. Bosnyak E, Kamson DO, Robinette NL, et al. (2016) Tryptophan PET predicts spatial and temporal patterns of post-treatment glioblastoma progression detected by contrast-enhanced MRI. J Neurooncol 126:317–325. [PubMed: 26514361]

29. Jeong JW, Juhasz C, Mittal S, et al. (2015) Multi-modal imaging of tumor cellularity and tryptophan metabolism in human gliomas. Cancer Imaging 15:10 [PubMed: 26245742]
30. Bosnyak E, Michelhaugh SK, Klinger NV, et al. (2017) Prognostic and molecular imaging biomarkers in primary glioblastoma. Clin Nucl Med 42:341–347. [PubMed: 28195901]
31. Juhasz C, et al. (2006) In vivo uptake and metabolism of alpha-[^{11}C]methyl-L-tryptophan in human brain tumors. J Cereb Blood Flow Metab 26:345–357. [PubMed: 16079785]
32. Kamson DO, et al. (2013) Differentiation of glioblastomas from metastatic brain tumors by tryptophan uptake and kinetic analysis: a positron emission tomographic study with magnetic resonance imaging comparison. Mol Imaging 12:327–337. [PubMed: 23759373]
33. Batista CE, et al. (2009) Imaging correlates of differential expression of indoleamine 2,3-dioxygenase in human brain tumors. Mol Imaging Biol 11:460–466. [PubMed: 19434461]
34. Kamson DO, et al. (2014) Increased tryptophan uptake on PET has strong independent prognostic value in patients with a previously treated high-grade glioma. Neuro Oncol 16:1373–1383. [PubMed: 24670609]
35. Bosnyak E, Barger GR, Michelhaugh SK, et al. (2018) Amino acid PET imaging of the early metabolic response during tumor-treating fields (TTFields) therapy in recurrent glioblastoma. Clin Nucl Med 43:176–179. [PubMed: 29261637]
36. Chakraborty PK, et al. (1996) A high-yield and simplified procedure for the synthesis of alpha-[^{11}C]methyl-L-tryptophan. Nucl Med Biol 23:1005–1008. [PubMed: 9004289]
37. Kikinis R, Pieper S (2011) 3D Slicer as a tool for interactive brain tumor segmentation. Conf Proc IEEE Eng Med Biol Soc 2011:6982–6984. [PubMed: 22255945]
38. Fedorov A, et al. (2012) 3D Slicer as an image computing platform for the Quantitative Imaging Network. Magn Reson Imaging 30:1323–1341. [PubMed: 22770690]
39. Mattes D, Haynor Dr, Vesselle H, Lewellen TK, Eubank W (2003) PET-CT image registration in the chest using free form deformations. IEEE Trans Med Imaging 22;120–128. [PubMed: 12703765]
40. Woodard HQ, Bigler RE, Freed B (1975) Letter: Expression of tissue isotope distribution. J Nucl Med 16:958–959.
41. Patlak CS, Blasberg RG, Fenstermacher JD (1983) Graphical evaluation of blood-to-brain transfer constants from multiple-time uptake data. J Cereb Blood Flow Metab 3:1–7. [PubMed: 6822610]
42. Bosnyak E, Kamson DO, Guastella AR,et al. (2015) Molecular imaging correlates of tryptophan metabolism via the kynurenine pathway in human meningiomas. Neuro-Oncol 17:1284–1292. [PubMed: 26092774]
43. Wen PY, Macdonald DR, Reardon DA, et al. (2010) Updated response assessment criteria for high-grade gliomas: response assessment in neuro-oncology working group. J Clin Oncol 28:1963–1972. [PubMed: 20231676]
44. Brandes AA, Franceschi E, Tosoni A, et al. (2008) MGMT promoter methylation status can predict the incidence and outcome of pseudoprogression after concomitant chemoradiotherapy in newly diagnosed glioblastoma patients. J Clin Oncol 26:2192–2197. [PubMed: 18445844]
45. Zhu X, McDowell MM, Newman WC, et al. (2017) Severe cerebral edema following nivolumab treatment for pediatric glioblastoma: case report. J Neurosurg Pediatr 19:249–253. [PubMed: 27858578]
46. Ranjan S, Quezado M, Garren N, et al. (2018) Clinical decision making in the era of immunotherapy for high grade-glioma: report of four cases. BMC Cancer 1;18:239.
47. Hassanzadeh C, Rao YJ, Chundury A, et al. (2017) Multiparametric MRI and [18F]fluorodeoxyglucose positron emission tomography imaging is a potential prognostic imaging biomarker in recurrent glioblastoma. Front Oncol 7:178. [PubMed: 28868256]
48. Antonios JP, Soto H, Everson RG, et al. (2017) Detection of immune responses after immunotherapy in glioblastoma using PET and MRI. Proc Natl Acad Sci U S A 114:10220–10225. [PubMed: 28874539]
49. Nandu H, Wen PY, Huang RY (2018) Imaging in neuro-oncology. Ther Adv Neurol Disord. 11:1756286418759865.
50. Opitz CA, Litzenburger UM, Sahm F, et al. (2011) An endogenous tumor-promoting ligand of the human aryl hydrocarbon receptor. Nature 478:197–203. [PubMed: 21976023]

51. Forouhar F, Anderson JL, Mowat CG, et al. (2007) Molecular insights into substrate recognition and catalysis by tryptophan 2,3-dioxygenase. Proc Natl Acad Sci USA 104:473–478. [PubMed: 17197414]

52. Basran J, Rafice SA, Chauhan N, et al. (2008) A kinetic, spectroscopic, and redox study of human tryptophan 2,3-dioxygenase. Biochemistry. 47:4752–4760. [PubMed: 18370401]

53. Giglio BC, Fei H, Wang M, et al. (2017) Synthesis of 5-[(18)F]Fluoro-alpha-methyl Tryptophan: New Trp based PET agents. Theranostics 7:1524–1530. [PubMed: 28529635]

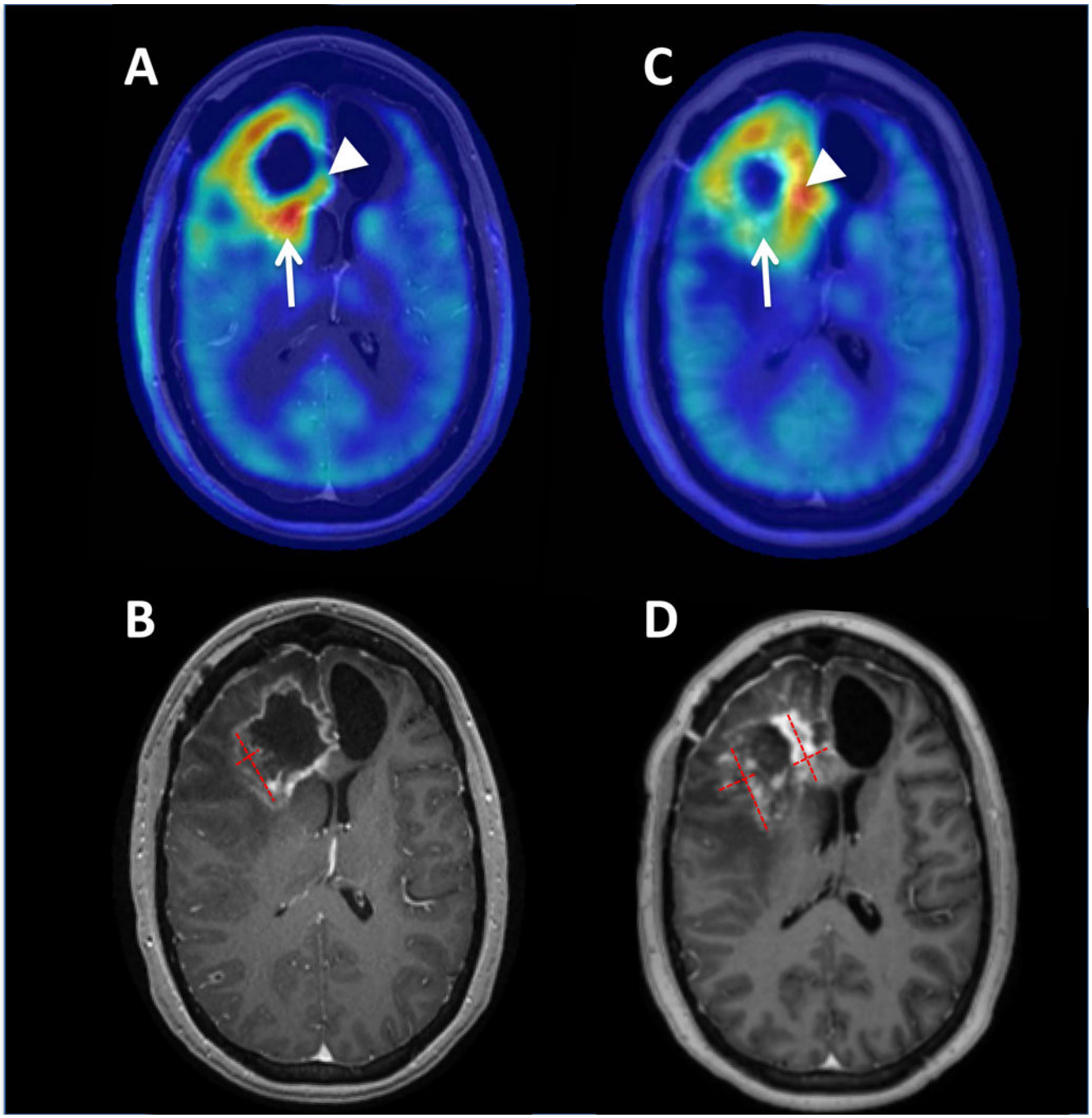

Figure 1.

Axial AMT-PET (**A, C**) and T1 post-contrast MR imaging (**B, D**) for patient 1. Pretreatment AMT-PET (**A**) and MRI (**B**) demonstrated an area of contrast enhancement with corresponding increased AMT uptake with maximum standardized uptake value (SUV) lesion/cortex ratio of 1.65 (arrow) in the posterior portion of the enhancing lesion, consistent with tumor recurrence. On-treatment AMT-PET (**C**) demonstrated an interval decrease of AMT uptake in this region with an SUV ratio of 1.48, suggesting that the observed expansion of MRI contrast enhancement (**D**) was pseudo-progression. However, other

regions of the tumor such as the medial frontal component (arrowheads) demonstrated an interval increase of AMT uptake (from 1.38 to 2.10 tumor/cortex ratio) consistent with tumor progression in the expanding contrast enhancing mass. Red dashed lines demonstrate the measurements of the baseline lesion and the expanded contrast-enhancing masses on the follow-up MRI (with the sum of the areas increasing from 4.8 cm^2 to 8.3 cm^2).

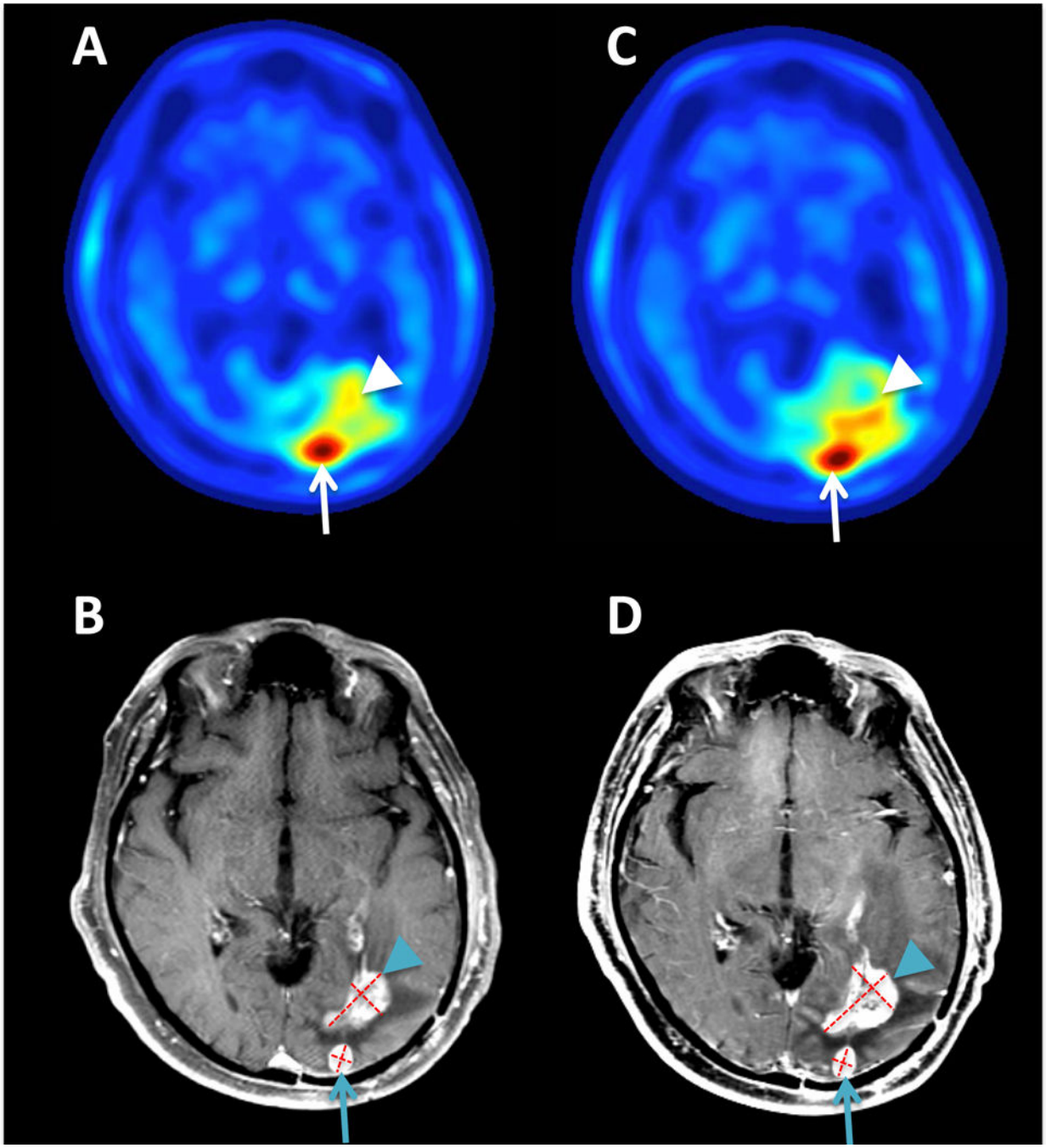

Figure 2.

Axial AMT-PET (**A, C**) and T1 post-contrast MR imaging (**B, D**) for patient 2. Pretreatment MRI showed two contrast-enhancing foci, and both foci showed high AMT SUV ratios on PET consistent with tumor recurrence, but the posterior lesion (arrows) showed substantially higher values (2.33) than the anterior-lateral mass (1.72, arrowheads). On-treatment and MRI (**D**) demonstrated an expansion of the contrast enhancing area (from 4.5 cm^2 to 6.0 cm^2) and associated hypointense region of the anterior mass, while the SUV ratio remained stable (1.76), suggesting pseudo-progression. The smaller, posterior nodule was stable on

repeat MRI (0.8 cm^2 and 0.9 cm^2 on baseline and follow-up, respectively) and showed a mild increase in AMT SUV ratios (to 2.5) on PET. AMT-PET kinetic analysis showed a decrease in tumor/cortex K-ratios in both lesions (2.04 to 1.6 in the anterior, and 1.27 to 1.14 in the posterior lesion), suggesting decreased AMT metabolism consistent with IDO enzyme blockade.

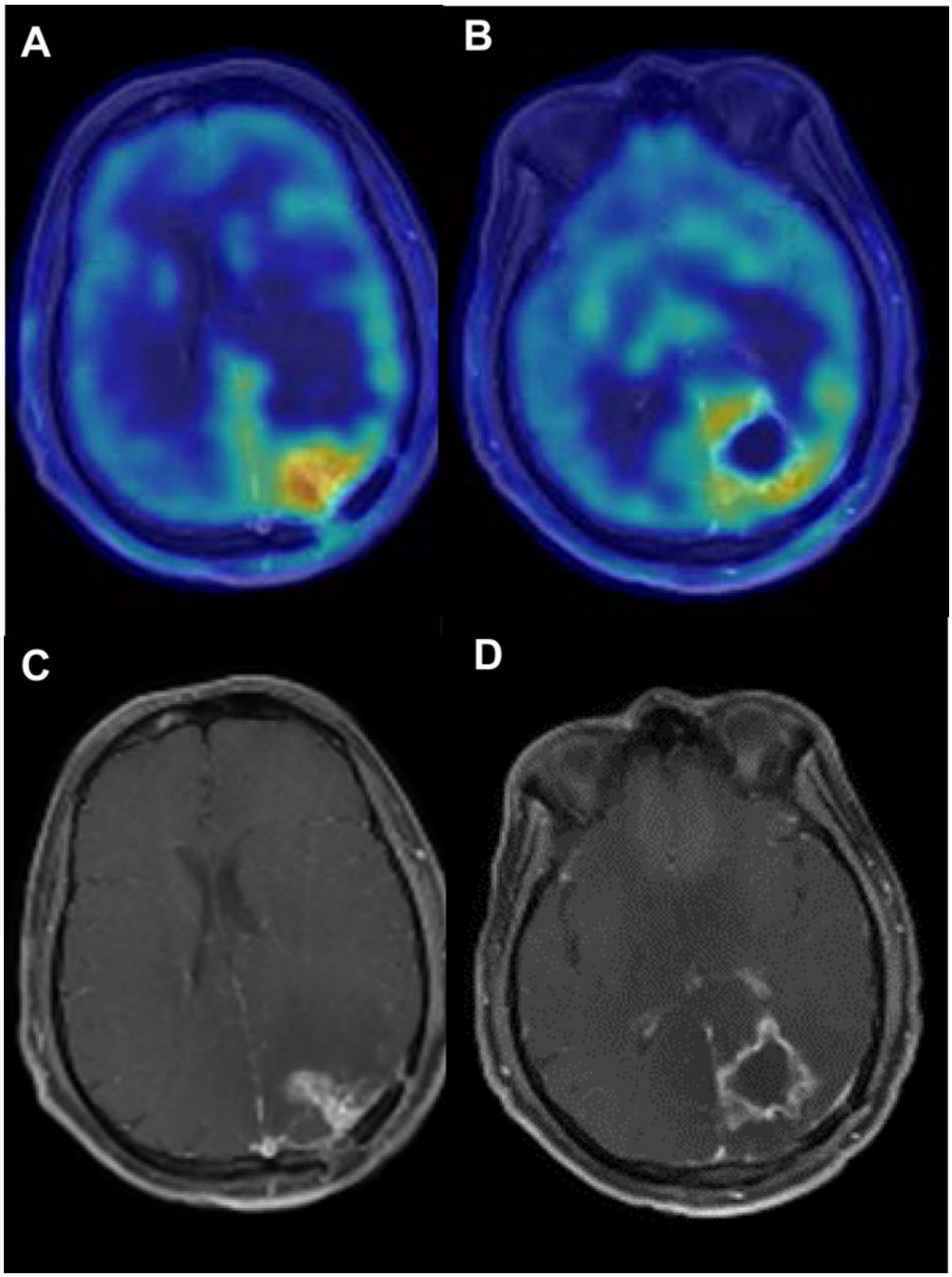

Figure 3.

Axial T1 post-contrast MRI and AMT-PET imaging for patient 3. Pretreatment imaging demonstrated AMT SUV ratios slightly above 1.65 in various tumor regions, consistent with active tumor and similar to baseline values seen in patient 1. No repeat AMT-PET was done due to rapid clinical progression during the first cycle of indoximod treatment.

Table 1

Patient	Age	Gender	Ethnicity	KPS*	IDH	MGMT promoter	Initial surgery	1st line treatment	2nd line treatment	Subsequent lines of treatment	OS**
1	36	female	white	100	wt	unmethylated	STR	RT/TMZ+TMZx4 cycles	Resection followed by indoximod+TMZx2 cycles	Bevacizumab+VB111; re-RT+TMZ+bevacizumab	5.5
2	63	male	white	100	wt	methylated	STR	RT/TMZ+TMZx3 cycles	Indoximod+TMZx3 cycles	Bevacizumab; durvalumab+tremiliimumab; lomustine+bevacizumab	24+
3	46	male	Hispanic	100	wt	unmethylated	GTR	RT/TMZ+TMZ/TTFx3 cycles	Indoximod+TMZx1 cycle	NA	2

KPS, Karnofsky Performance Score; IDH, isocitrate dehydrogenase; wt, wild type; MGMT, methyl-guanine methyl transferase; OS, overall survival; TMZ, temozolomide; TTF, tumor treating fields; RT, radiation therapy; NA, not applicable.

*at time of initiation of indoximod+temozlomide

**measured in months from after initiation of indoximod with temozolomide.